

# A Real-Time On-Chip Algorithm for IMU-Based Gait Measurement

Shenggao Zhu, Hugh Anderson, and Ye Wang

School of Computing, National University of Singapore, Singapore  
{zhusheng,hugh,wangye}@comp.nus.edu.sg

**Abstract.** This paper presents a real-time and on-chip gait measurement algorithm used in our Gait Measurement System (GMS). Our GMS is a small foot-mounted device based on an Inertial Measurement Unit (IMU), which contains an accelerometer and a gyroscope. The GMS can compute spatio-temporal gait parameters in real-time and transmit them to a remote receiver. Measured gait parameters include cadence, velocity, stride length, swing/stance ratio and so on. The algorithm is optimized to run in a ATmega328 microprocessor with only 2kB data memory. During a walking session, each stride is recognized instantaneously, and the stride length and other parameters are computed at the same time. Although inexpensive components are utilized, the algorithm achieves high accuracy, with an average stride length error smaller than 3%, and error in total walking distance less than 2%.

**Keywords:** Gait Measurement, Algorithm, IMU, Real-Time, On-Chip.

## 1 Introduction

The primary motivation for our gait measurement system (GMS) was in the Healthcare field, in clinical therapy and rehabilitation of people suffering from walking difficulties, such as Parkinson's disease (PD) patients and stroke victims. Many of their symptoms may be hard to treat, or even have no cure, and physiotherapy is commonly used to improve the patients' quality of life. For clinical use and rehabilitation, inertial measurement units (IMUs) have been widely utilized in various assistive and/or monitoring systems. Researchers have already developed IMU-based devices for detection and prevention of Freezing of Gait (FOG) symptoms of PD patients [1], fall detection [2], and general gait parameters measurement [3,4].

A specific music therapy method for these patients is known as Rhythmic Auditory Stimulation or RAS [5]. To facilitate and automate the music therapy procedures, our research group is developing a RAS-based gait training system, which has two subsystems. One is a gait measurement subsystem to detect the walking cadence in real-time. Another subsystem is the tempo-based music search engine, which can retrieve a proper song whose tempo is related to the patient's target walking cadence [6]. Patients can follow the rhythm of the selected songs while having gait training. Our IMU-based GMS is a small

foot-mounted device to measure cadence and other gait parameters, as well as assess the patient's improvement over time. The components of our GMS prototype include an ATmega328 based microcontroller board (Arduino Pro Mini), an IMU, a radio frequency module (RFM12B), and a 3.7 volt Lithium-ion battery. The IMU is a combo board of a 3-axis accelerometer (ADXL345) and a 3-axis gyroscope (ITG-3200). The whole device measures 34mm×18mm×11mm in size and weighs 9g (battery included).

Recently there have been intensive investigations into sensor-based gait measurement as well as dead reckoning [7]. However, some gait measurement approaches rely on the sensor fusion of IMU and other sensors, like a magnetometer [8] or Foot Force Sensor (force sensitive resistors) [3]. Other IMU-based approaches require remote computers to calculate gait parameters [9,10]. Another study does use on-chip computing [4], but only the frequency domain algorithm is used, and it cannot measure velocity or stride length, which are important parameters for gait analysis. By contrast, our GMS only uses simple and cheap inertial sensors, and performs on-chip gait analysis in real-time. A wireless communication interface is also integrated into the GMS to work with applications in remote computers or mobile devices like smart phones. Therefore our GMS can operate in both indoor and outdoor scenarios with relatively level ground, such as a corridor or a level park road. This is much more convenient than the traditional machine vision based gait measurement.

Algorithms for IMU-based gait measurement can be generally grouped into three categories: abstraction model, gait model and direct integration. Abstraction model based algorithms do not study the specific walking biomechanics, but use neural networks and machine learning methods to abstract and estimate the walking patterns [11]. Algorithms using gait models make use of the derived kinematic information from some predefined models, such as modeling two legs as the two sides of an isosceles triangle during walking [12]. However, the accuracy of both methods is limited because they rely on models which vary between people. The resultant training or setup phase for these models can take a long time, rendering systems based on these algorithms less convenient to use.

Algorithms based on direct integration are relatively accurate and simple. The main idea is to measure walking acceleration through inertial sensors, so that the velocity and stride length can be derived by single and double integration of acceleration [3,7,9,13]. This kind of algorithms need to handle noises and sensor drifts carefully, using methods like zero velocity update (ZUPT) [10]. As reported in literature, the best accuracy result achieved with relatively expensive sensors is about 2% error in walking displacement [7,9,10].

In our GMS, the algorithm is also based on direct integration. The detailed data processing procedures will be described in this paper. Although our GMS prototype is built up with cheap components, the average stride length error is smaller than 3%, and the error of total walking distance measurement is less than 2%. These accuracy results are comparable with those achieved by the use of expensive sensors.

## 2 Stride Cycle Detection

### 2.1 Data Preprocessing

The inertial coordinate system  $XYZ$  of a foot-mounted IMU is represented in Fig. 1. The GMS is carefully attached to the heel or shoe so that the IMU's  $yz$ -plane stays approximately parallel to the user's forward direction during the walking session. In practice, this condition is easy to ensure. The algorithm assumes that people walk on relatively level ground, in both outdoor and indoor scenarios. Therefore, we can use acceleration in  $y$ -axis ( $a_y$ ) and  $z$ -axis ( $a_z$ ) as well as angular rate around  $x$ -axis ( $\omega_x$ ) to fully describe the foot motion. We need to calculate the horizontal acceleration ( $a_h$ ) and perpendicular acceleration ( $a_p$ ) in the global reference frame. The raw sensor data of an example walking session are shown in Fig. 2. As can be seen from the figure,  $a_y$ ,  $a_z$  and  $\omega_x$  are the three most significant signals among all the six sensor readings. In the following data processing, only these three signals are used.

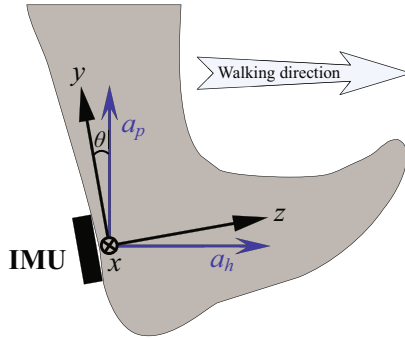


**Fig. 1.** Illustration of the IMU coordinate system  $XYZ$  and the walking direction

After the GMS is assembled, the IMU sensors must be calibrated once, recording the zero offset and sensitivity of each axis. For the accelerometer, the calibration is straightforward by using gravitational acceleration  $\mathbf{g}$ . For each axis, we measure  $+1 g$  and  $-1 g$  values  $V_{1g}$  and  $V_{-1g}$ . Thus the acceleration sensitivity  $S_a$  and zero offset  $V_{offset}$  can be obtained by (1)

$$\begin{cases} S_a = (V_{1g} - V_{-1g})/(2g), \\ V_{offset} = (V_{1g} + V_{-1g})/2. \end{cases} \quad (1)$$

For the gyroscope, the zero offset is simply the data output when the hardware is stationary. The sensitivity of the gyroscope is determined by rotating the gyroscope about each axis through a range of constant angular rates. In our case, we found the sensitivity recorded in the gyroscope specification sheet was accurate, so there was no need for calibrating the sensitivity of the gyroscope.

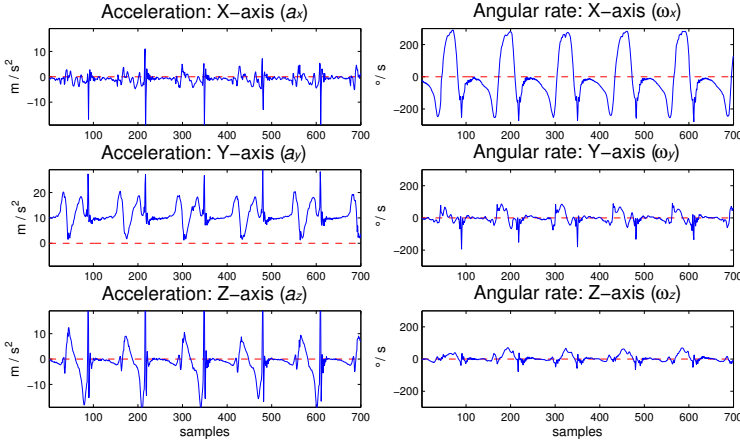


**Fig. 2.** IMU sensor outputs during walking gait

After the sensors are properly calibrated, the raw sensor readings ( $V_{raw}$ ) can be correctly converted to signals ( $V_{signal}$ ) in units of  $m/s^2$  (accelerometer) or  $^\circ/s$  (gyroscope), as expressed by (2).

$$V_{signal} = (V_{raw} - V_{offset})/Sensitivity. \quad (2)$$

Once the sensor data are collected and calibrated, we need to filter out the noise. Usually the walking frequency is lower than 2 Hz, thus we can set the stop frequency of the low-pass filter at  $5 \sim 10$  Hz.

## 2.2 Stride Cycle Detection

People’s walking motion is a series of alternate *stances* and *swings*, separated by the Toe-off and Heel-strike points (Fig. 3). In order to conduct in-depth and real-time gait analysis, each stride cycle should be recognized and extracted from the continuous walking data. According to a widely accepted “zero velocity assumption” [14], there is a certain *zero point* during the stance phase where the acceleration, velocity and angular rate of a foot-mounted IMU can all be regarded as zero. This is especially the case when the IMU is attached to the heel. In our GMS model, a complete stride is defined as the interval between two successive zero points.

Our real-time algorithm realizes intelligent stride cycle detection through a series of time-varying thresholds combined with a sliding window technique. Since the toe-off and heel-strike points correspond to sharp fluctuations of foot movement, they are identified by the negative impulses of the angular rate waveform, as shown in Fig. 4. A toe-off point (point A in Fig. 4) is confirmed only if the following three conditions are satisfied: (1) point A is the local minimum of  $\omega_x$  and smaller than a certain low threshold; (2) a local maximum point B after

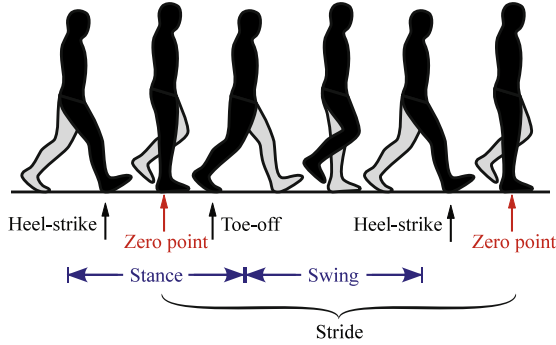


**Fig. 3.** Illustration of the gait phase and characteristic points (right foot)

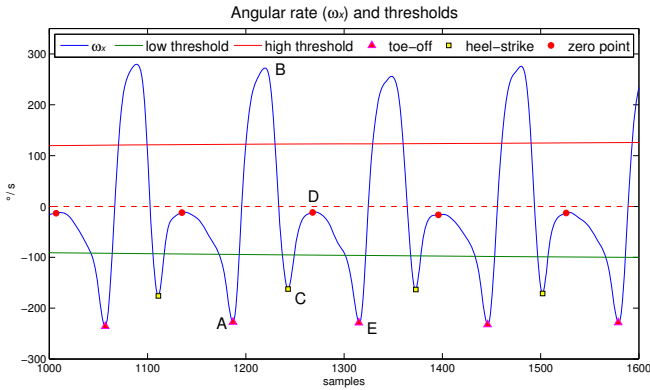


**Fig. 4.** Stride cycle detection based on angular rate

point A is bigger than a certain high threshold; and (3) both point A and B are within a sliding window with a size of about half a stride cycle. Similarly, a heel-strike point C is verified after the thresholds and sliding window conditions are met. During the process, the thresholds and window size are dynamically changed according to the waveform of  $\omega_x$ , so that the algorithm can fit different walking patterns automatically.

The interval between heel-strike point C and toe-off point E is the stance phase. During the middle part of stance, the angular rate is relatively close to zero, indicating very slow foot movement. Therefore we define zero point as the vertex (point D) during stance phase, which is generally the closest point to zero. By identifying these characteristic points, we can recognize the swing and stance phases as well as every stride cycle, and this lays the foundation for further gait parameters analysis.

### 3 Gait Parameters Measurement

In our gait parameters measurement algorithm, a stride cycle is the fundamental unit for analysis, and a series of stride cycles can be processed one by one, independently. After each stride cycle has been processed, related parameters are updated immediately. This property enables our real-time implementation of the algorithm on a limited memory microprocessor.

#### 3.1 Temporal Parameters Measurement

With the correct stride cycle detection, we can easily obtain the following temporal gait parameters.

**1. Cadence:** Cadence means the number of steps per minute. This is an essential gait parameter for many applications, such as cadence-based music retrieval and recommendation. The average cadence of a walking session can be computed as the total steps divided by the time duration, while the instantaneous cadence is given by the following Equation

$$c = 60 \cdot \frac{f}{n} \cdot 2, \quad (3)$$

where  $f$  is the sensor sampling frequency and  $n$  is the number of sample points within the current stride (one stride consists of two sequential steps).

**2. Swing/Stance Ratio:** By recognizing the toe-off and heel-strike points, we can collect and compare the swing time ( $T_{sw}$ ) and the stance time ( $T_{st}$ ). The swing/stance ratio (SSR) is defined as  $SSR = T_{sw}/T_{st}$ . Since the  $T_{sw}$  of one foot is related with the  $T_{st}$  of another foot, SSR can reflect the gait symmetry of two feet to some extent. This parameter may be used to assess the walking ability of a particular person over time.

As our group is cooperating with a local hospital, we have also observed that many patients have difficulty in holding gait balance: because of physical impairment or lack of confidence, they tend to put more weight of the body on one foot than on another, leading to asymmetric gait patterns. When a patient with gait imbalance walks in a straight line, the stride length of both feet should be close, but usually one leg would move faster than another. To assess the gait balance, we can compare the velocities of both feet, or the SSRs; the closer they are, the more balanced the gait is.

#### 3.2 IMU Orientation Angle

In order to obtain horizontal acceleration ( $a_h$ ), we need to project the measured acceleration in the IMU's coordinate system to a global reference frame, and thus the IMU's orientation angle  $\theta$  (the angle between the IMU's y-axis and the  $a_p$  direction, as illustrated in Fig.1) has to be calculated first. The IMU orientation angle is a core parameter for gait analysis, and its accuracy has a considerable effect on the velocity and stride length.

Based on the “zero velocity assumption”, we assume that the foot has no movement at zero points, so that only the gravitational acceleration is measured by the accelerometer. Therefore we can estimate the IMU’s initial orientation angle  $\theta_0$  by (4)

$$\theta_0 = \arctan\left(\frac{a_{z0}}{a_{y0}}\right), \quad (4)$$

where  $a_{y0}$  and  $a_{z0}$  are the y-axis and z-axis acceleration at zero point, respectively. Many papers assume that  $\theta_0$  is also zero if the device is properly attached [9]. However, this will introduce a further measurement error.

During the walk, the IMU rotates about the x-axis. The total rotation angle  $\theta_1(t)$  is the integral of angular rate  $\omega_x$  over time:

$$\theta_1(t) = \int_0^t \omega_x d\tau. \quad (5)$$

Hence the IMU’s instantaneous orientation angle is  $\theta(t) = \theta_0 + \theta_1(t)$ .

Assume that  $\theta(t)$  has a value of  $\theta_{end}$  at the end of a stride (which is also a zero point).  $\theta_{end}$  is most likely different from  $\theta'_0$  calculated by (4) at the beginning of the next stride, which will lead to a gap in the  $\theta(t)$  waveform. This integration drift is usually caused by noise in the gyroscope output combined with accumulating numerical integration errors. To compensate for this drift, we developed a linear de-drift method, which resets  $\theta_{end}$  to  $\theta'_0$  and adjusts other intermediate  $\theta(t)$  values linearly. The new values after de-drift are computed as

$$\theta_d(t) = \theta(t) + \frac{t}{T}(\theta'_0 - \theta_{end}), \quad (6)$$

where  $T$  is the total time duration of the stride.

We choose the “linear” adjustment because integration is a linear transformation and we assume that the accumulated rate of errors is an approximately constant value. The orientation angle after de-drift is smooth throughout, as shown in Fig. 5.

### 3.3 Spatial Parameters Measurement

After obtaining the IMU’s orientation angle, the following gait parameters can be derived from the sensor data.

**1. Velocity.** Given the accelerometer readings in y-axis ( $a_y$ ) and z-axis ( $a_z$ ), the IMU’s horizontal acceleration ( $a_h$ ) and perpendicular acceleration ( $a_p$ ) are calculated by (7)

$$\begin{bmatrix} a_h \\ a_p \end{bmatrix} = \begin{bmatrix} -\sin(\theta) & \cos(\theta) \\ \cos(\theta) & \sin(\theta) \end{bmatrix} \begin{bmatrix} a_y \\ a_z \end{bmatrix} - \begin{bmatrix} 0 \\ g \end{bmatrix}, \quad (7)$$

in which  $g$  is the gravitational acceleration. In our GMS model, we assume people walk on level ground, and thus the horizontal acceleration and velocity are the

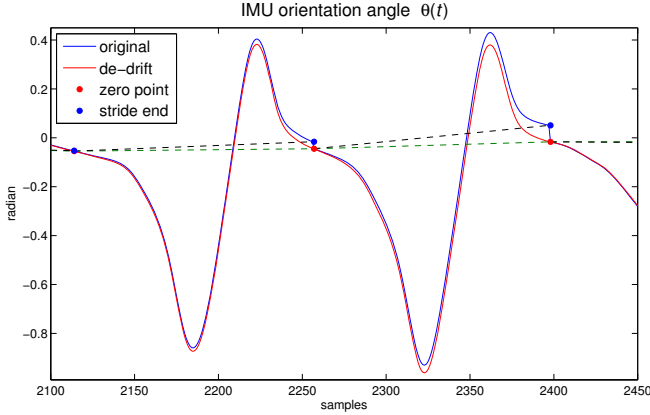


**Fig. 5.** Linear de-drift for IMU orientation angle

most significant. Since the initial velocity at the beginning of a stride is zero, the horizontal velocity  $v(t)$  is the single integral of  $a_h$ .

$$v(t) = \int_0^t a_h d\tau. \quad (8)$$

Similarly, a linear de-drift method is performed on  $v(t)$  which resets its value at the end of the stride to zero.

**2. Stride Length:** Stride length is the integral of velocity over the period of a stride cycle, given by

$$s = \int_0^T v(t) dt. \quad (9)$$

The derived horizontal acceleration, velocity and stride length are presented in Fig. 6. The stride length ground-truth (actual values) collected by camera are included to compare with the estimated values. The total walking distance is the sum of all stride lengths in a walking session. An important aspect affecting stride length measurement is the selection of the starting point and ending point of the stride cycle, or the zero points. One improper zero point may affect its adjacent stride lengths, but has less effect on the total walking distance. This is the reason why the error (2% in relative percentage) of walking distance is usually smaller than that of stride length (3%).

**3. Stride Regularity:** We use the percentage of the standard deviation of stride length in relation to the average stride length to represent the stride regularity of a walking session. A small stride regularity indicates a stable, regular walking pattern.

Other useful statistics (e.g., averages, maximums) can be derived from the above calculated parameters.

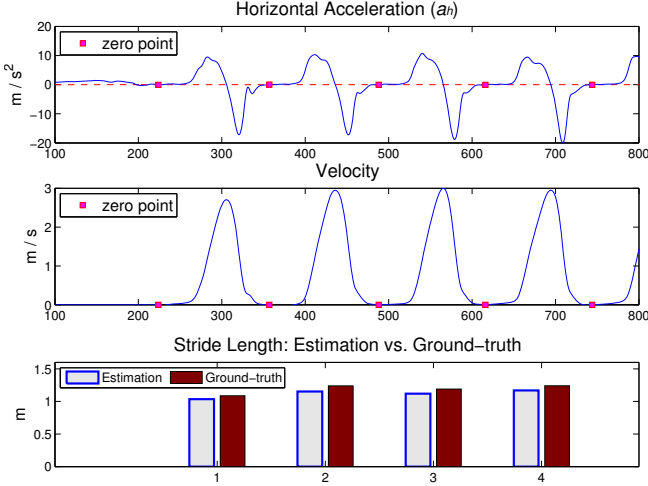


Fig. 6. Spatial parameters measurement: acceleration, velocity and stride length

### 3.4 Error Model

Although sensor calibration and de-drift methods are used, the stride length computed by the above algorithm tends to be smaller than the ground-truth (See the examples in Fig. 6). We closely observed the walking process, and confirmed that the bottom of the foot has zero velocity during the period around zero point. However, the IMU’s velocity at zero point is slightly higher than zero because the IMU has a distance from the ground and can rotate slowly as the heel bends forward. As a result, resetting the velocity to zero finally leads to an underestimated stride length.

In order to compensate for this measurement error, we use a simple linear regression to model the relationship between estimated stride length and the ground-truth (Fig. 7). In the experiments, we collected a series of strides with different walking speed and stride lengths. The total stride count is 701 (346 for training and 355 for testing). Based on the regression result, we adjust the originally estimated stride length by (10).

$$S_{adjusted} = 0.99 * S_{estimated} + 0.08. \quad (10)$$

The mean value, standard deviation (STD) and root mean squared error ( $RMSE = \sqrt{\sum (V_{measurement} - V_{ground-truth})^2 / N}$ ) are used to assess the stride length before and after adjustment, as shown in Table 1. In the training set, the originally computed stride length has a mean error of 7 cm (6%), and its RMSE is 7.8 cm. After adjustment by (10), the RMSE is reduced to 3 cm. The testing strides also have similar improvement after adjustment, and finally achieve high accuracy.

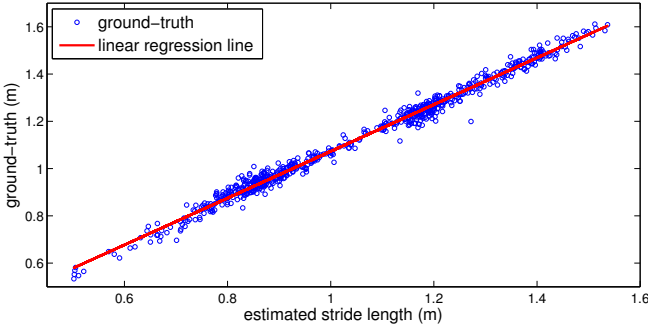


**Fig. 7.** Linear regression for stride length

**Table 1.** Comparison of stride length before and after adjustment (unit: m)

		Mean	STD	RMSE
Training strides (346)	ground-truth	1.13	0.20	/
	estimated	1.06	0.20	0.078
	adjusted	1.13	0.20	0.022
Testing strides (355)	ground-truth	1.11	0.24	/
	estimated	1.04	0.24	0.074
	adjusted	1.11	0.23	0.025

## 4 Experiments and Results

To evaluate the performance of the GMS measurement algorithm, walking experiments were conducted on five subjects (2 female and 3 male, all in their twenties). All subjects were healthy and had no gait abnormalities. Subjects were asked to walk along a 20-meter-long corridor with the GMS attached to the left heel. The corridor floor was marked to collect ground-truth by camera.

We designed four different walking patterns according to the walking speed: Slow, Normal, Fast and Mixed. The Mixed pattern was a combination of the first three patterns in which the walking speed varied among different strides. For each pattern, 10 walking sessions were completed and all the subjects were involved. No significant differences were found among subjects.

The mean value, RMSE and %RMSE (the ratio of RMSE to the average of ground-truth) are used to assess the accuracy of measured parameters like stride length and total walking distance of each session. Detailed experimental results are listed in Table 2 (cadence, velocity and swing/stance ratio are all average values).

In all the experiments, every stride cycle was recognized correctly. Compared with the Mixed pattern, the other three patterns had more stable gait (as can be seen from the stride regularity), and accordingly achieved higher accuracy in stride length and walking distance measurement. In general, we can conclude that the stride length error is less than 3%, and walking distance error less than 2%. These accuracy results are sufficient for many common applications.

**Table 2.** Experiment results

		Slow	Normal	Fast	Mixed
Sessions		10	10	10	10
Total strides		209	159	137	196
Cadence (step/min)		66	90	103	78
Velocity (m/s)		0.52	0.92	1.23	0.65
Swing/stance ratio		0.61	0.75	0.83	0.61
Stride regularity		5.7%	4.7%	5.8%	20.6%
Stride length	Mean(m)	0.94	1.23	1.43	1.01
	RMSE(m)	0.022	0.024	0.022	0.027
	%RMSE	2.3%	1.9%	1.6%	2.7%
Walking distance	Mean(m)	19.6	19.5	19.6	19.8
	RMSE(m)	0.17	0.11	0.14	0.32
	%RMSE	0.8%	0.5%	0.7%	1.6%

## 5 Conclusion and Future Work

We have presented the gait measurement algorithm for our small and low cost GMS. It has two important features: (1) real-time computation, which is critical for many context-aware and healthcare related applications; and (2) low complexity and memory usage, so that it can be implemented in a small microprocessor of an embedded system. In practice the GMS achieved accurate measurements, with an average stride length error smaller than 3%, and error in total walking distance less than 2%, which is comparable to systems based on much more expensive components. Other measurements such as gait cadence and stride regularity are also captured, useful in a clinical environment.

A companion paper [15] describes our efforts to reduce the current consumption of the GMS to a level which allows for months of continuous usage. We are working on improving the algorithm so that the GMS can work accurately with any orientation mounted on the foot (at the moment it must be mounted with a particular orientation). We are cooperating with a local hospital and will use this GMS with patients to evaluate the effectiveness of the system.

**Acknowledgements.** The work was supported by Singaporean MOE grant R-252-000-463-112. We thank the anonymous reviewers for their constructive comments.

## References

1. Bachlin, M., Plotnik, M., Roggen, D., Maidan, I., Hausdorff, J., Giladi, N., Troster, G.: Wearable Assistant for Parkinson's Disease Patients With the Freezing of Gait Symptom. *IEEE Transactions on Information Technology in Biomedicine* 14(2), 436–446 (2010)

2. Lee, Y., Kim, J., Son, M., Lee, M.: Implementation of Accelerometer Sensor Module and Fall Detection Monitoring System based on Wireless Sensor Network. In: 29th Annual International Conference of the IEEE Engineering in Medicine and Biology Society, EMBS 2007, pp. 2315–2318 (August 2007)
3. Bamberg, S., Benbasat, A., Scarborough, D., Krebs, D., Paradiso, J.: Gait Analysis Using a Shoe-Integrated Wireless Sensor System. *IEEE Transactions on Information Technology in Biomedicine* 12(4), 413–423 (2008)
4. Yang, C.C., Hsu, Y.L., Shih, K.S., Lu, J.M., Chan, L.: Real-time gait cycle parameters recognition using a wearable motion detector. In: 2011 International Conference on System Science and Engineering, ICSSE, pp. 498–502 (June 2011)
5. Thaut, M.H., McIntosh, G.C., Rice, R.R., Miller, R.A., Rathbun, J., Brault, J.M.: Rhythmic auditory stimulation in gait training for Parkinson's disease patients. *Movement Disorders* 11(2), 193–200 (1996)
6. Li, Z., Xiang, Q., Hockman, J., Yang, J., Yi, Y., Fujinaga, I., Wang, Y.: A music search engine for therapeutic gait training. In: Proceedings of the International Conference on Multimedia, MM 2010, pp. 627–630. ACM, New York (2010)
7. Ojeda, L., Borenstein, J.: Non-GPS navigation for security personnel and first responders. *Journal of Navigation* 60(3), 391–407 (2007)
8. Facchinetti, T., Savioli, A., Goldoni, E.: Design and development of a real-time embedded inertial measurement unit. In: Proceedings of the 2010 ACM Symposium on Applied Computing, SAC 2010, pp. 491–495. ACM, New York (2010)
9. Li, Q., Young, M., Naing, V., Donelan, J.: Walking speed estimation using a shank-mounted inertial measurement unit. *Journal of Biomechanics* 43(8), 1640–1643 (2010)
10. Sabatini, A., Martelloni, C., Scapellato, S., Cavallo, F.: Assessment of walking features from foot inertial sensing. *IEEE Transactions on Biomedical Engineering* 52(3), 486–494 (2005)
11. Song, Y., Shin, S., Kim, S., Lee, D., Lee, K.: Speed Estimation From a Tri-axial Accelerometer Using Neural Networks. In: 29th Annual International Conference of the IEEE Engineering in Medicine and Biology Society, EMBS 2007, pp. 3224–3227 (August 2007)
12. Miyazaki, S.: Long-term unrestrained measurement of stride length and walking velocity utilizing a piezoelectric gyroscope. *IEEE Transactions on Biomedical Engineering* 44(8), 753–759 (1997)
13. Alvarez, J., Gonzalez, R., Alvarez, D., Lopez, A., Rodriguez-Uria, J.: Multisensor Approach to Walking Distance Estimation with Foot Inertial Sensing. In: 29th Annual International Conference of the IEEE Engineering in Medicine and Biology Society, EMBS 2007, pp. 5719–5722 (August 2007)
14. Peruzzi, A., Croce, U.D., Cereatti, A.: Estimation of stride length in level walking using an inertial measurement unit attached to the foot: A validation of the zero velocity assumption during stance. *Journal of Biomechanics* 44(10), 1991–1994 (2011)
15. Zhu, S., Anderson, H., Wang, Y.: Reducing the Power Consumption of an IMU-Based Gait Measurement System. In: Weisi, L., Dong, X., Anthony, H., Jianxin, W., Ying, H., Jianfei, C., Mohan, K., Ming-Ting, S. (eds.) PCM 2012. LNCS, vol. 7674, pp. 105–116. Springer, Heidelberg (2012)